Journal of Applied Pharmaceutical Science 2025. Article in Press
Available online at http://www.japsonline.com
DOI: 10.7324/JAPS3.2025.231503
ISSN 2231-3354

Therapeutic effects of *Bajakah kalalawit* extract (*Uncaria gambir* Roxb.) in HCl/ethanol-induced rats as an animal model in acute gastritis: UHPLC MS/MS profiling and *in vivo* approach with *in silico* validation

Aulia Andi Mustika[1*], Lina Noviyanti Sutardi[2], Andriyanto Andriyanto[1], Sharon Aurellia[1], Anisa Rahma[2], Rahayu Woro Wiranti[3], Andhika Yudha Prawira[4], Derajat Taruno Jati[2], Ekowati Handharyani[3], Setyanto Tri Wahyudi[5,6]

[1]Division of Pharmacology and Toxicology, School of Veterinary Medicine and Biomedical Sciences, IPB University, Bogor, Indonesia.
[2]Division of Veterinary Pharmacy, School of Veterinary Medicine and Biomedical Sciences, IPB University, Bogor, Indonesia.
[3]Division of Pathology, School of Veterinary Medicine and Biomedical Sciences, IPB University, Bogor, Indonesia.
[4]Research Center for Applied Zoology, Research Organization for Life Science and Environment, National Research and Innovation Agency (BRIN), Cibinong, Indonesia.
[5]Bioinformatics Study Program, IPB University, Bogor, Indonesia.
[6]Tropical Biopharmaca Research Center, IPB University, Bogor, Indonesia.

ARTICLE HISTORY
Received on: 12/04/2024
Accepted on: 30/05/2024
Available Online: XX

Key words:
Acute gastritis, active compounds, *Bajakah kalalawit*, ***Uncaria gambir***.

ABSTRACT

Uncaria gambir Roxb., a plant known for its health-promoting properties and rich in bioactive compounds, offers an alternative treatment for acute gastritis. This research involved the approach of network pharmacology, pathway analysis, and molecular docking to predict signaling pathways of *Bajakah kalalawit* (***Uncaria gambir* Roxb.**) extract in treating acute gastritis. The results were validated through an *in vivo* experiment using 25 rats, divided into normal healthy group, negative control, positive control, and treatment groups, and administered with the extract at a dose of 100 and 200 mg/kg BW. The rats were induced with acute gastritis using HCl/ethanol. *In vivo* parameters include the severity of gastric lesions, histopathological examination, ELISA assay, and immunohistochemistry to measure the levels of pro-inflammatory cytokines, including interleukin (IL)-6 and tumor necrosis factor (TNF)-α. Network pharmacology proved that there was a significant connection between the active secondary metabolite of the extract and acute gastritis-related genes. Although molecular docking proved that these compounds have limited potential in directly inhibiting TNF-α and IL-6, the *in vivo* findings nonetheless proved the gastroprotective effect, where the administered groups showed reduced gastric lesions and retained mucosal integrity through histopathological staining. The results of immunohistochemistry and ELISA proved that the extract modulated the levels of TNF-α and IL-6.

INTRODUCTION

Gastritis is commonly described as a disease resulting from an inflammation of the stomach lining, also known as gastric mucosa [1]. Gastritis can be classified into chronic and acute, depending on the duration of symptoms. Acute gastritis is a short-term inflammation of the stomach lining, typically lasting less than a month, mostly just 1 or 2 days [2]. The rise in gastritis prevalence is linked to unhealthy lifestyles, such as lack of physical activity, poor diet, obesity, smoking, and the excessive consumption of alcohol [3].

In this age of time, alcohol has become one of the leading causes of acute gastritis, eroding the mucosal lining of the stomach [4]. Mucosal inflammation causes the disruption of gastric mucosal

*Corresponding Author
Aulia Andi Mustika, Division of Pharmacology and Toxicology, School of Veterinary Medicine and Biomedical Sciences, IPB University, Bogor, Indonesia. E-mail: auliaandi @ apps.ipb.ac.id

barrier, secretion of gastric acid and pepsin, along with mucosal damage caused by the release of inflammatory cells that infiltrate the gastric lining [5]. Mucosal inflammation is associated with the release of pro-inflammatory cytokines, such as tumor necrosis factor (TNF)-α, interleukin 6 (IL-6), and cyclooxygenase-2 (COX-2) [6,7], with IL-6 and TNF-α as specific inflammatory cytokines associated with acute gastritis inflammation [8].

Gastritis treatment covers from the use of medications to more invasive procedures, such as surgery, in severe cases. Medications commonly used to treat gastritis depend on the type and severity of symptoms. These include antacids, proton pump inhibitors (PPIs), and H-2 receptor antagonists, all of which work to reduce stomach acid and promote healing of the gastric mucosa, through different mechanisms of action [9,10]. Unfortunately, the use of these medications tends to have negative side effects, especially in long-term use or individuals with organ dysfunctions, such as liver and kidney disease [11]. Other than that, individuals may experience side effects such as fatigue, diarrhea, vomiting, headache, and dizziness [12]. This has led current research to center on finding alternatives by using plant-based extracts, relying on their active components to manage gastritis.

Uncaria gambir Roxb., commonly known as gambir, is a plant native to Kalimantan, Central, and Southern Sumatra, Indonesia. Several studies have proven useful compounds in gambir, such as alkaloids, flavonoids, and tannins, and the plant has been considered as an excellent source of antioxidant compounds [13]. Traditionally, local communities have used gambir to treat various conditions, such as physical wounds, ulcers, asthma, headache, diabetes, rheumatism, urinary tract issues, dysentery, gastrointestinal diseases, and even cancer [14]. Although gambir is recognized for treating various health issues, there is currently no research demonstrating its effectiveness in alleviating acute gastritis.

Uncaria gambir Roxb., known for its benefits in treating various health conditions, has not yet been scientifically proven to alleviate acute gastritis. However, gambir is known to contain flavonoid, phenolic, and antioxidant compounds [15]. They offer great potential in alleviating acute gastritis by reducing and preventing inflammation. Hence, this study aimed to investigate the gastroprotective activity of *Bajakah kalalawit* ***(Uncaria gambir Roxb)*** extract analysis of active compound using chromatographic analysis and *in vitro* and *in silico* methods along with network pharmacology to better understand its mechanism of action, findings were then verified the efficacy further observed through *in vivo* study using rat model.

MATERIALS AND METHODS

Preparation of *B. kalalawit* extract

Bajakah kalalawit was purchased from Berau Regency, South Kalimantan, with its identity already confirmed by a taxonomist. A voucher specimen is stored in the National Research and Innovation Agency at the Herbarium Bogoriense, Directorate of Scientific Collection Management, BRIN Cibinong, Indonesia, with certificate number B-2770/II.6.2/IR.01.02/8/2024. The roots were washed under running tap water to eliminate debris, and then air-dried at room temperature. Crude extract was obtained by drying plants for 24 hours, at the temperature of 45°C, and grounded into fine powder using a grinder. The powder was extracted twice with 70% (v/v) methanol for 24 hours each time. The extract was then filtered to remove any residue, and the supernatant was evaporated to a semi-dry state using a vacuum evaporator. The semi-dried residue was stored at −80°C to solidify any remaining moisture. The extract was stored in a dark bottle at the temperature of −20°C until the time of the experiment.

Apparatus and LC-HRMS condition

Metabolite compounds in *B. kalalawit* extract were identified using ultra-high-performance liquid chromatography-high-resolution mass spectrometry. Liquid Chromatography-High Resolution Mass Spectrometry (LC-HRMS) analysis was conducted according to Windarsih *et al.* [16]. The analysis was performed using liquid chromatography equipment (Thermo Scientific™ Vanquish™ UHPLC Binary Pump) and Orbitrap high-resolution mass spectrometry (Thermo Scientific™ Q Exactive™ Hybrid Quadrupole-Orbitrap™ High-Resolution Mass Spectrometer). Liquid chromatography was performed using a Thermo Scientific™ Accucore™ Phenyl-Hexyl 100 mm × 2.1 mm ID × 2.6 µm analytical column. The mobile phases consisted of MS-grade water with 0.1% formic acid (A) and MS-grade methanol with 0.1% formic acid (B), both were applied in a gradient flow, at 0.3 ml/min. Mobile phase B started from 5% and increased to 90% over 16 minutes, then held at 90% for 4 minutes, and returned to 5% after 25 minutes. The column temperature was maintained at 40°C, with an injection volume of 3 µl. Untargeted screening was conducted using full MS/dd-MS2 acquisition in both positive and negative ionization modes. Nitrogen was used as the sheath gas, auxiliary gas, and sweep gas at settings of 32, 8, and 4 arbitrary units, respectively. The spray voltage used was 3.30 kV, with a capillary temperature of 320°C, and the auxiliary gas heater was set to 30°C. The mass scan range was 66.7–1,000 m/z, with a resolution of 70.000 for full MS and 17.500 for dd-MS2 in positive ionization mode. The system was managed using XCalibur software (Thermo Scientific, Bremen, Germany).

Mass identification of metabolites was performed using Compound Discoverer™ 3.2 software (Thermo Scientific, USA), employing an untargeted metabolomics workflow. Peak extraction filters were applied using MzCloud and ChemSpider databases, with mass annotations ranging from −5 to 5 ppm.

2,2 diphenly 1-picrylhydrazyl analysis

2,2 diphenly 1-picrylhydrazyl (DPPH) analysis was conducted using UV-Vis spectrophotometric method. The crude extract of *B. kalalawit* was measured for its antioxidant activity using DPPH. A total of 3.5 ml of DPPH with a concentration of 25 ppm in methanol was mixed with 0.5 ml of the extract, starting from the concentration of 4, 8, 12, 16, 20 µg/ml. The mixture was incubated at room temperature for 20 minutes. The optical density of the mixture was taken at 517 nm. DPPH scavenging activity was measured with the formula as follows:

$$\text{DPPH scavening activity } (\%) = \left[\frac{\text{ABS}_{\text{control}} - \text{ABS}_{\text{sample}}}{\text{ABS}_{\text{control}}}\right] \times 100$$

$ABS_{control}$: Absorbance of DPPH + methanol
ABS_{sample}: Absorbance of DPPH + *Bajakah kalalawit* extract

Network pharmacology analysis

Active compounds were classified into secondary metabolites classes, such as flavonoids, alkaloids, isoflavones, coumarins, phenols, and terpenes. These compounds were further observed to explore their potential on inhibiting inflammation related to acute gastritis.

Swiss Target Prediction Database (http://www.swisstargetprediction.ch) was used to obtain putative targets of active compounds that have been chosen. Acute gastritis-related targets were searched in the GeneCards database (https://www.genecards.org) with "acute gastritis" as the keyword.

The targets of active compounds and gastritis were input into the website Bioinformatics & Evolutionary Genomics. The same targets of the two were considered interaction targets. The compound-target network was established using the software Cytoscape 3.10.2.

The construction of the PPI network was performed after finding a common target via the STRING dataset. There were 105 common targets found. Data analysis mode was set to "multiple proteins," and the species were limited to "*Homo sapiens*."

The common interaction targets for *U. gambir* and gastritis were submitted into the ShinyGO website for gene ontology (GO) analysis. The analysis includes biological process, cellular components, molecular functions, and pathways. The top 20 results based on false discovery rate (FDR) were exported into charts.

Molecular docking

Proteins chosen for the molecular docking simulation were TNF-α (PDB ID: 2AZ5) and IL-6 (PDB ID: 1ALU), downloaded through RCSB PDB (https://www.rcsb.org/). Meanwhile, the ligands used were the active secondary metabolites of *B. kalalawit* extract from the result of LC-HRMS [17,18].

Downloaded proteins were separated from their co-crystal ligands and other unrelated components using *BIOVA Discovery Studio* 2016. Omeprazole was used as a comparison ligand in the simulation [19]. The structure of the secondary metabolite compound and omeprazole were obtained through PubChem, continued by minimization of energy using *PvRX* 0.8, with the result saved in the extension of *pdbqt. The proteins were then input into software as macromolecules [20,21].

The validation of molecular docking was carried out to confirm that the molecular docking method that would be used on the test ligands is appropriate. The validity of molecular docking could be observed from the value of root mean standard deviation (RMSD) < 2 Å. The validation process includes the creation of a grid box and redocking of TNF-α (PDB ID: 2AZ5) and IL-6 (PDB ID: 1ALU), with each co-crystal ligand using PyRx 0.8. [20,21]. The co-crystal ligands and grid box used on the proteins are shown in Table 1.

Molecular docking on the test ligands of *B. kalalawit* extract was performed after the validation. Molecular docking was performed using PyRx 0.8. The determination of the best compounds on inhibiting TNF-α and IL-6 was based on the affinity energy from the result of test ligand molecular docking compared to the native ligands of the proteins. Chemical bonding analysis in the form of hydrogen bonds and interactions was conducted by visualizing the result of molecular docking using Ligplot+ 2.2.9 and PyMOL software [20,18].

Table 1. Gridbox of molecular docking validation.

Proteins (PDB ID)	Native ligands	Grid box					
		Center			Dimension (Å)		
		X	*y*	*z*	*x*	*y*	*z*
TNF-α (2AZ5)	307	8.21	67.88	19.83	15.16	14.48	16.83
IL-6 (1ALU)	TLA	−7.31	−13.30	0.13	10.42	10.37	10.43

Molecular dynamics simulation method

Molecular dynamics simulation consists of two parts: the relaxation part and the production run part.

Methods of relaxation

Through nine successive steps, the relaxation phase methodically gets the system ready for molecular dynamics simulations. Initially, we restrict all other atoms, optimize their locations, and minimize the energy of water molecules and ions. The system is then heated progressively over 1 ns at constant number of particles volume and temperature from 100 to 298 K, with velocities carefully assigned using a Maxwell–Boltzmann distribution to ensure stability. After heating, the system relaxes for one false discovery rate (FDR) (NPT), enabling density changes. Then, to allow for incremental flexibility, the constraints are gradually lowered from 10 kcal/mol·Å² on all atoms to only the backbone atoms. In a series of 1 ns simulations at constant pressure, the limits on the backbone are slowly decreased (from 10 to 1 to 0.1 kcal/mol·Å²), until there are no limits left in the final 1 ns relaxation step. This methodical process guarantees that the system stabilizes and finds equilibrium, making it ready for further production simulations.

Methods of production runs

By using the hydrogen mass repartitioning (HMR) method, which lets us use a longer time step while keeping things stable, the main phase of the run lasted 200 nanoseconds with a time step (dt) of 0.004 ps. The system was not subjected to any constraints during this phase. Simulation frames were saved at intervals of 2,500 steps to enable detailed trajectory analysis. We used periodic boundary conditions in the simulation to imitate the effects of a large amount of solvent, and the SHAKE algorithm was used to keep the bonds with hydrogen atoms stable. Using the Langevin dynamics thermostat with a lambda value of 1.0 to effectively regulate temperature fluctuations, the production run was conducted in the NPT ensemble to maintain constant pressure and temperature. The system's dynamic behavior under almost physiological settings was reliably and accurately sampled thanks to this configuration.

In vivo validation

Animal preparation

This study used 10-week-old male Wistar albino rats, weighing between 180 and 200 g. The number of samples was five rats per group based on the power analysis calculation assuming a large effect size using the formula according to Arifin *et al.* [22]. This calculation suggested a minimum of 2–4 animals per group to detect significant effects. Additionally, the sample size selection also considered the 3Rs principles (Replacement, Reduction, Refinement) in animal experimentation. Although larger sample sizes ($n = 6$) are commonly used, several previous studies with similar gastritis models have also used five animals per group and successfully detected significant differences [23,24]. However, we acknowledge that a larger sample size would improve the robustness of the research and will be considered in future studies.

The rats were obtained from the laboratory animal management unit at the School of Veterinary Medicine and Biomedical Sciences, IPB University. The rats were kept in standard rat cages at the temperature of 23°C ± 2°C, with a 12-hour light-dark cycle and humidity maintained between 35% and 60%. Rats had free access to food and water. All experimental procedures were approved by the Animal Ethics Committee (KEH) of IPB University, under approval number 237/KEH/SKE/VIII/2024.

Induction of acute gastritis using ethanol/HCl

The experiment followed a completely randomized design. Twenty-five rats were randomly assigned to five groups, each group containing five rats. The groups were divided into normal healthy group, negative control group (administered with saline solution), positive control group, administered with omeprazole at a dose of 20 mg/kg BW [25], and treatment groups administered with *B. kalalawit* extract at a dose of 100 and 200 mg/kg BW.

One and a half hours after the treatments, all rats (except those in the negative control group) were administered with 5 ml/kg BW of a mixture of 0.15 M HCl and 60% ethanol solution following the method of Nam and Choo [6] and Al-Quraishy *et al.* [23]. The rats were euthanized 90 minutes later using a combination of xylazine and ketamine. The stomachs were immediately sampled and fixed in 4% buffered neutral formalin solution for 1 hour. Each stomach was then incised along the greater curvature, and photographed using iPad Air 5th Generation (Apple, China).

Measurement of gastric lesion surface area

The surface area of the gastric lesion was measured using ImageJ software and expressed as a percentage (%), obtained by comparing the lesion's surface area to the total surface of each gastric sample.

Histopathological and immunohistochemical analysis

The gastric samples, fixed in 10% neutral buffered formaldehyde, were processed for histopathology, embedded in paraffin, sectioned at 4 mm thickness, and stained with hematoxylin and eosin (H&E) for morphological evaluation of the villi and subsequent image analysis.

Samples used for immunochemistry were gastric samples from the rats. Immunohistochemical analysis was done using anti-IL-6 antibody ab9324 and anti-TNF-α antibody ab34674 produced by Abcam plc, Cambridge, UK.

ELISA assay

Samples used for ELISA assay were serum collected from the rats, and the measurement was duplicated for each sample. Pro-inflammatory cytokines TNF-α and IL-6 determination were conducted with an ELISA Fine Test kit, manufactured by Wuhan Fine Biotech Co., Ltd (ISO9001). Total protein content of the supernatant was determined based on the Lowry method [26].

Acute toxicity

The ethanolic extract of *B. kalalawit* was given to mice at predetermined dosage levels of 5, 50, 300, and 2,000 mg/kg body weight. An observational approach was utilized to determine the starting dose, which aimed to elicit detectable toxicity while avoiding serious adverse effects or death. The following doses were modified according to observed signs of toxicity or lethality, with this procedure continuing until identifying either a dose producing clear toxicity or demonstrating no adverse effects at the maximum tested concentration. The *B. kalalawit* ethanolic extract was delivered as a single administration through oral gavage via gastric intubation after subjects underwent overnight feed restriction before treatment. Six mice were used for each dosage group. Assessment protocols encompassed routine clinical observation, weekly weight monitoring, and postmortem gross examination.

Statistical analysis

The data are shown as mean ± standard error of the mean. Data were first analyzed for their normality and homogeneity using the Shapiro–Wilk and Levene test. Data that did not show normality and homogeneity were analyzed using the Kruskal–Wallis method, with group comparisons conducted using the Dunn test in R software version 2024.09.0+375. A significance level of $p < 0.05$ was used to determine the significance difference.

RESULTS

Screening of *U. gambir* Roxb. extract active compounds

A total of 70 active compounds were identified through LC-HRMS analysis of *U. gambir* Roxb. root extract as shown in Figure 1. The compounds were subsequently screened into different classes to further assess their potential efficacy in treating acute gastritis. The screening process identified three key active compounds of *U. gambir* Roxb. root extract based on its secondary metabolites, including alkaloids, flavonoids, and coumarins, as shown in Table 1.

Active compound analysis has proven that *U. gambir* Roxb. extract contains three main active compounds (Alkaloids, flavonoids, and coumarins).

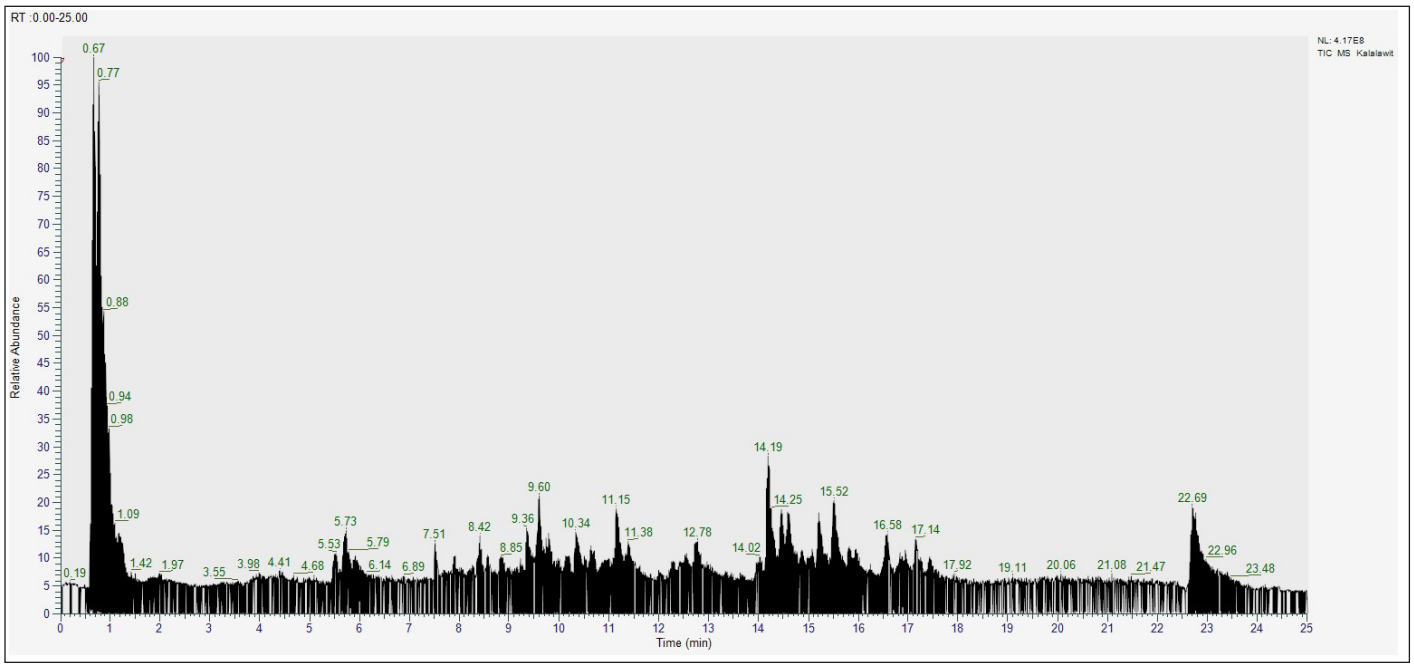

Figure 1. The result of LC-HRMS analysis of *B. kalalawit* extract active compounds.

Table 2. Identification of *U. gambir* Roxb. root extract potential active compounds [15,16].

No	Name	Formula	Annot. DeltaMass [ppm]	Calc. MW	RT [min]	Category
1	Catechin	$C_{15}H_{14}O_6$	−0.35	290.0789	4.309	Flavonoids
2	(+)-Procyanidin B2	$C_{30}H_{26}O_{12}$	−1.34	578.1417	4.216	Flavonoids
3	7-hydroxy-6-methoxy-2H-chromen-2-one	$C_{10}H_8O_4$	−0.9	192.0421	5.566	Coumarin
4	4-Methoxy DMT	$C_{13}H_{18}N_2O$	−1.07	218.1417	3.992	Alkaloids
5	N,N-Dimethyltryptamine	$C_{12}H_{16}N_2$	−1.13	188.1311	3.577	Alkaloids
6	1-(14-methylhexadecanoy) pyrrolidine	$C_{21}H_{41}NO$	−2,11	323.3181	16.513	Alkaloids

Table 3. The result of DPPH analysis of *B. kalalawit* extract.

No	Parameters	Unit	Result
1	Antioxidant (IC_{50})	mg/l	9.14

DPPH analysis

DPPH analysis was conducted to find out the antioxidant activity of *B. kalalawit* extract. The result of DPPH analysis is shown in Table 3.

Based on the result of DPPH analysis, *B. kalalawit* extract shows the level of antioxidant with an IC_{50} value of 9.14 mg/l.

Network construction and analysis

All the active compounds in Table 2 were uploaded to the Swiss Target Prediction Database to obtain their gene targets. A total of 431 active component-related gene targets were found. The disease targets were obtained through the GeneCards database, and 1,435 genes were found.

Disease targets with the target compounds were compared to find their common targets that is the potential anti-acute gastritis targets of *U. gambir* Roxb. Common targets were obtained through the Bioinformatics & Evolutionary Genomics website using a Venn diagram. A total of 105 common targets were found, as shown in Figure 2A.

A network of common targets shared between the active compounds and potential targets was developed. This initial network mapping helps to identify and visualize the direct interactions between active compounds identified in *U. gambir* Roxb. and their corresponding targets associated with anti-acute gastritis targets. This sequential approach allows for a more structured and comprehensive analysis of the molecular mechanism involved (Fig. 2B).

PPI was constructed by inputting 105 common targets into the STRING database to obtain relevant protein–protein interaction, and with the obtained proteins, PPI network of *U. gambir* Roxb. and acute gastritis-related targets was visualized using Cytoscape 3.10.2. The network comprises 104 nodes and 1,280 edges (Fig. 2C).

Based on Figure 2C, the most highly connected targets in the network were IL-6 and TNF-α, which can interact with 104 proteins, highlighting their significant roles in molecular-scale mechanisms of underlying acute gastritis and potential therapeutic signaling pathways affected by the active compounds in the extract of *U. gambir* Roxb. root.

GO analysis was conducted to find out the GO term in biological process, cellular components, molecular functions, and KEGG pathways to find out the active compounds' actions in the molecular level.

Based on the result of network PPI (Fig. 3), the target protein of IL-6 and TNF-α holds a crucial role in gastritis. The result of enrichment GO also proved that the target proteins of gastritis is involved in the process of the transduction of cell signaling and the regulation of cell death. The cellular components of these proteins include aggresomes, inclusion bodies, membranes, and vesicles. Molecular function mainly consists of binding activity of the protein. Several pathways show that the target proteins work in cancer pathway, TNF-α, P13K-Akt, and AGE-RAGE signaling pathways.

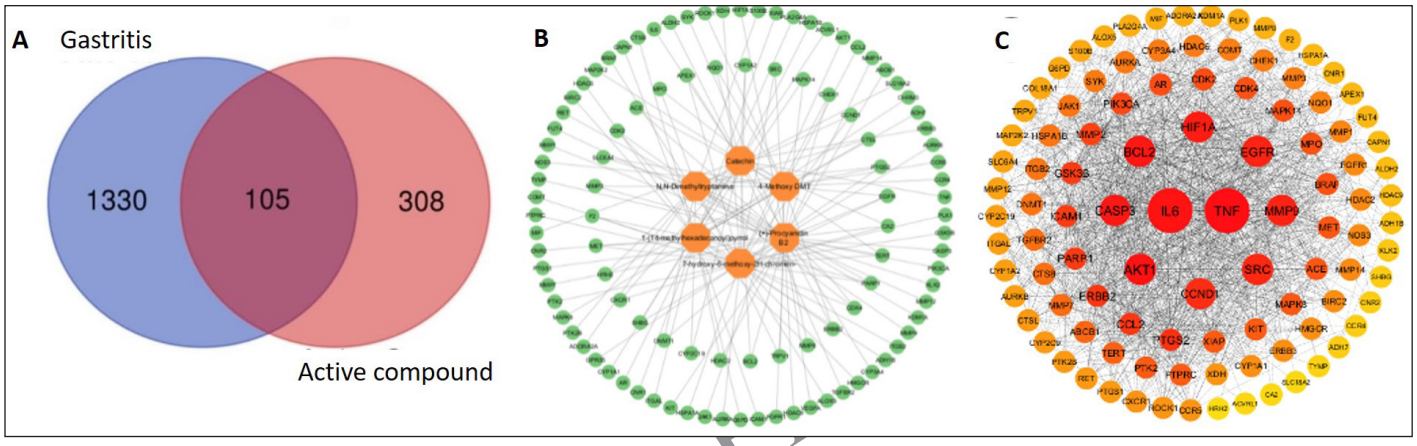

Figure 2. Results of network construction and analysis. A: Venn diagram illustrating the relationship between active compounds and anti-acute gastritis targets. Active compound-related targets (blue circle); Anti-gastritis targets (red circle); Overlapping section: potential anti-acute gastritis targets that are affected by the active compounds. B: The network construction of compound-target network of potential targets and active compounds. Orange circles represent active compounds; green circles represent common targets. C: The PPI network of potential targets related to acute gastritis. Smaller circles represent potential targets; larger circles indicate a larger degree value.

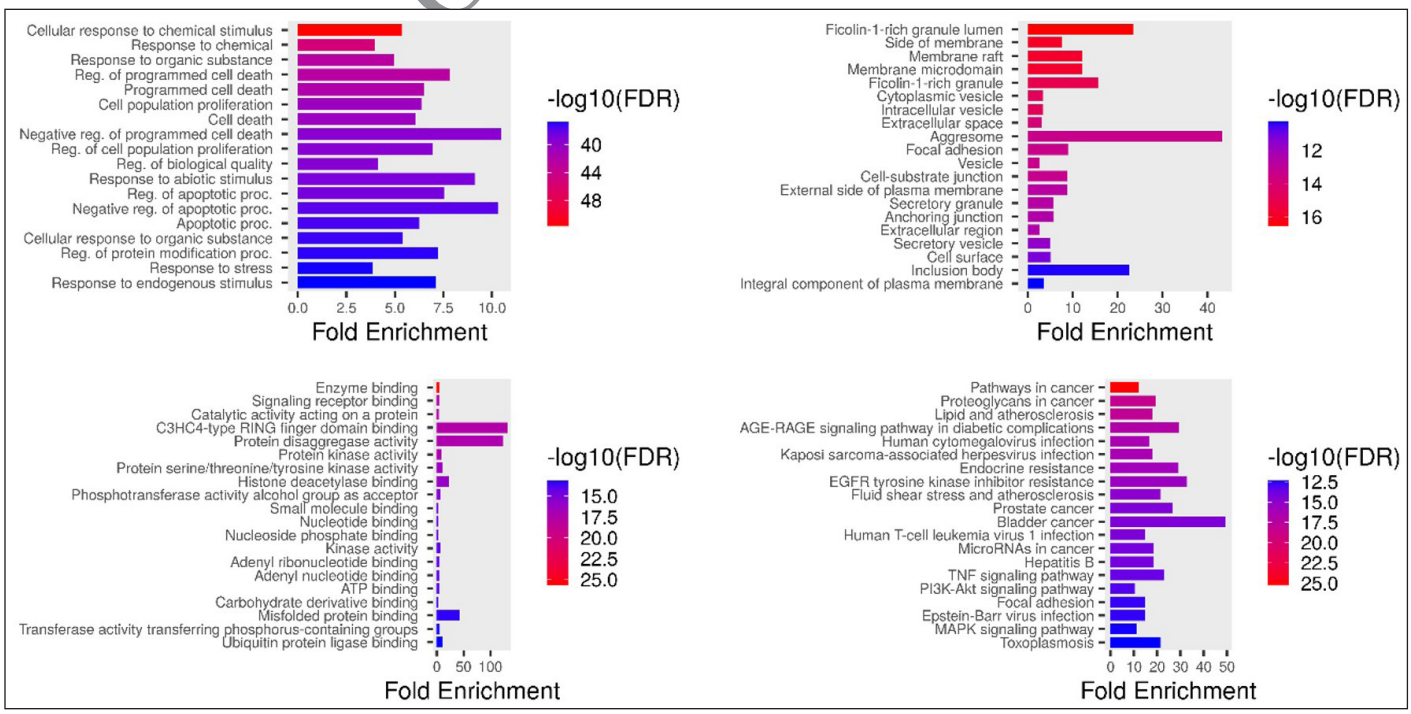

Figure 3. GO terms of *U. gambir.* (A) GO term, biological process, (B) GO term, cellular component, (C) GO term, molecular function, (D) GO term KEGG pathways.

Molecular docking

The results of the molecular docking validation are represented with the value of RMSD < 2 Å. The result of TNF-α and IL-6 molecular docking with their representative co-crystal showed the value of RMSD as 0,726 Å, 0,895 Å, and 1,942 Å, respectively. Based on the result, the values of RMSD are still below 2 Å, proving that the method used for *B. kalalawit* extracts test ligands as appropriate.

Molecular docking of TNF-α (PDB ID: 2AZ5) on the chosen ligands showed that all ligands had greater affinity energy value compared to omeprazole, which is −7.1 kcal/mol. The test ligand of 7-hydroxy-6-methoxy-2H-chromen- showed the greatest value of affinity energy, closest to omeprazole, with the value of −6.0 kcal/mol.

Molecular docking of IL-6 (PDB ID: 1ALU) on the test ligands of *B. kalalawit* extract showed that one compound had a more negative affinity energy value compared to omeprazole, with the value of −4.3 kcal/mol. The test ligands of 7-hydroxy-6-methoxy-2H-chromen- is the test ligand with the highest affinity energy value, which is −4.8 kcal/mol. Meanwhile, the molecular interaction from the visualization showed that omeprazole and test ligands of *B. kalalawit* extract showed molecular interaction in the form of hydrogen bond and hydrophobic interaction. The affinity energy is shown in Table 4 and the visualizations of the interaction of TNF-α and IL-6 with *B. kalalawit* extract active compounds are shown in Figure 4. Hydrogen bonds and hydrophobic interactions are shown in Table 5.

Molecular dynamic simulation

In this study, molecular dynamics simulation is used to prove the binding stability of previous molecular docking results. Therefore, we only show distance analysis data, including protein–ligand distance, ligand pose distance relative to the reference ligand position, and end-to-end distance. In addition, we also provide binding energy data from the calculation results using molecular mechanics/generalized born surface area (MMGBSA), and we present it in the form of a time series. Presentation in the form of time series allows us to see the binding energy at any time.

Distance analysis on protein TNF alpha

The interaction of the four ligands, 1-(14-methylhexadecanoyl)pyrrolidine, 7-hydroxy-6-methoxy-2H-chromen-2-one, N,N-dimethyltryptamine, and omeprazole, with TNF-alpha protein, shows different binding stability. Ligand 1-(14-methylhexadecanoyl)pyrrolidine and omeprazole

Table 4. Affinity energy of *B. kalalawit* extract secondary metabolites.

Proteins	Ligands	Affinity energy (kkal/mol)
TNF-α (PDB ID: 2AZ5)	Omeprazole (control ligand)	−7.1
	7-hydroxy-6-methoxy-2H-chromen-	−6.0
	1-(14-methylhexadecanoyl)pyrrolidine	−5.9
	N,N-Dimethyltryptamine	−5.7
IL-6 (PDB ID: 1ALU)	Omeprazole (control ligand)	−4.3
	7-hydroxy-6-methoxy-2H-chromen-	−4.8
	1-(14-methylhexadecanoyl)pyrrolidine	−4.3
	N,N-Dimethyltryptamine	−3.7

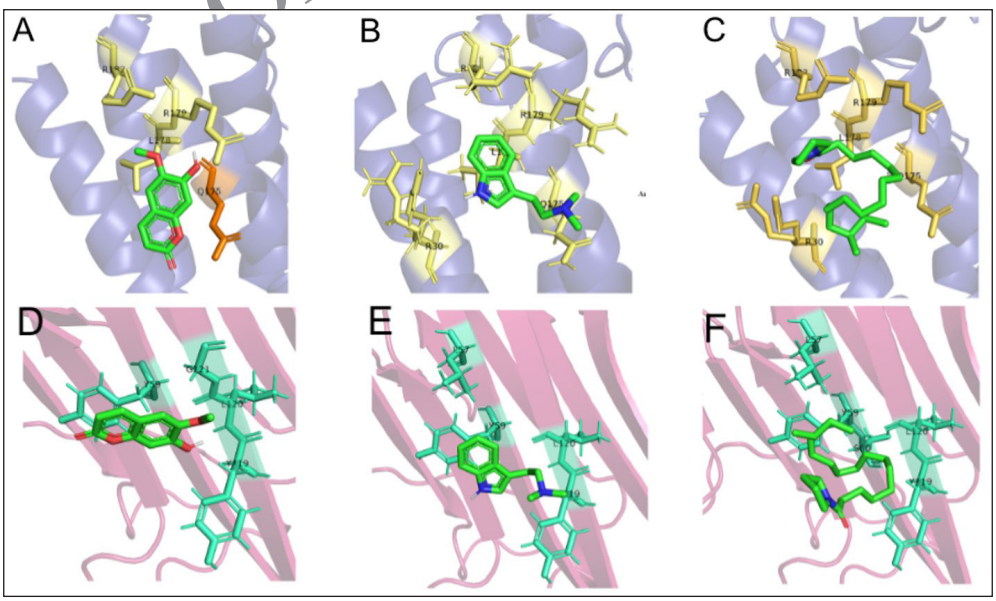

Figure 4. 3D visualization of the interactions between pro-inflammatory cytokines TNF-α and IL-6 toward the active compounds of *B. kalalawit* extract. A: Interaction between IL-6 and 7-hydroxy-6-methoxy-2H-chromen-; B: Interaction between IL-6 and N,N-Dimethyltryptamine; C: Interaction between IL-6 and 1-(14-methylhexadecanoyl) pyrrolidine); D: Interaction between TNF-α and 7-hydroxy-6-methoxy-2H-chromen-; E: Interaction between TNF-α and N,N-Dimethyltryptamine; F: Interaction between TNF-α and 1-(14-methylhexadecanoyl)pyrrolidine). Hydrophobic interactions could be seen in yellow for IL-6 and cyan for TNF-α.

Table 5. Molecular interaction of native ligands and test ligands of *B. kalalawit* extract's active compounds with TNF-α and IL-6.

Ligands	Hydrogen bonds	Hydrophobic interactions
TNF-α (PDB ID: 2AZ5)		
Omeprazole (native ligand)	Tyr151	Tyr57, Tyr59
7-hydroxy-6-methoxy-2H-chromen-	-	Tyr59, Tyr119, Leu120, Gly121
1-(14-methylhexadecanoyl)pyrrolidine	-	Tyr57, Tyr59, Ser60, Tyr119, Leu120
N,N-Dimethyltryptamine	-	Tyr57, Tyr59, Tyr119, Leu120
IL-6 (PDB ID: 1ALU)		
Omeprazole (control ligand)	-	Arg30, Gln175, Leu178, Arg179, Arg182
7-hydroxy-6-methoxy-2H-chromen-	Gln175	Leu178, Arg179, Arg182
1-(14-methylhexadecanoyl)pyrrolidine	-	Arg30, Gln175, Leu178, Arg179, Arg182
N,N-Dimethyltryptamine	-	Arg30, Gln175, Leu178, Arg179, Arg182

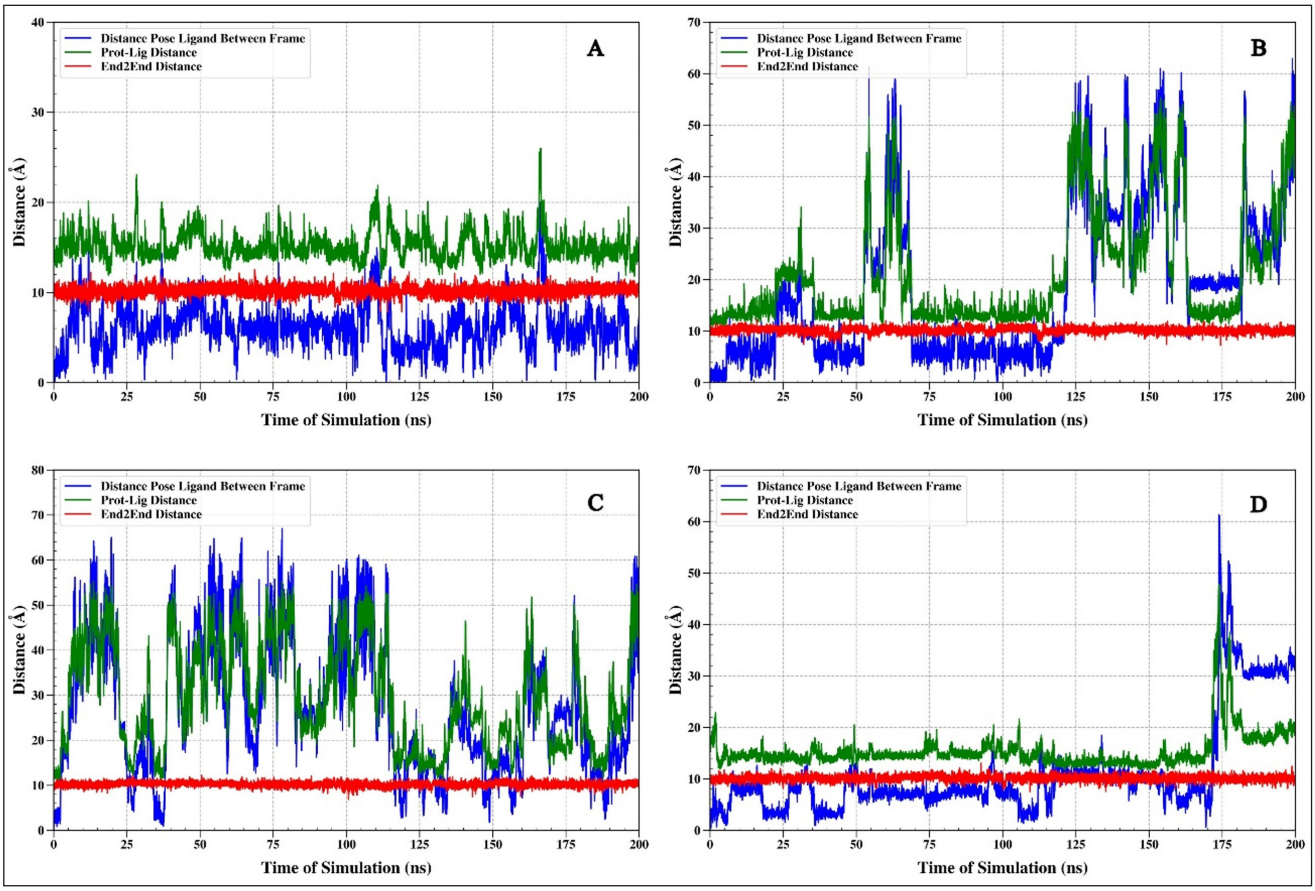

Figure 5. The analysis shows the distance between the TNF-α protein and the ligand (green), the end-to-end distance (red), and the relative position of the ligand (blue) during the 200 ns simulation. Complex IL6-1-(14-methylhexadecanoyl)pyrrolidine (A), IL6-7-hydroxy-6-methoxy-2H-chromen-2-one (B), IL6-N, N-Dimethyltryptamine (C), and IL6-omeprazole (D).

have relatively little fluctuation in distance dynamics (Fig. 5A and D). The relative pose of the ligand ranges from 5 to 10 Å, and as a result, the distance of the protein–ligand ranges from 15 Å to the ligand 1-(14-methylhexadecanoyl)pyrrolidine. This ligand shows good stability of distance fluctuation for 200 ns. The end-to-end graph of the protein, when bound to each ligand (Fig. 5), indicates that the red graph demonstrates significant stability around 10 Å. The data indicate that the overall architecture of the protein remains largely unchanged when interacting with the ligand.

MMGBSA: binding energy analysis on protein TNF alpha

The results from the MMGBSA binding energy analysis show a pattern that supports the results of the distance analysis

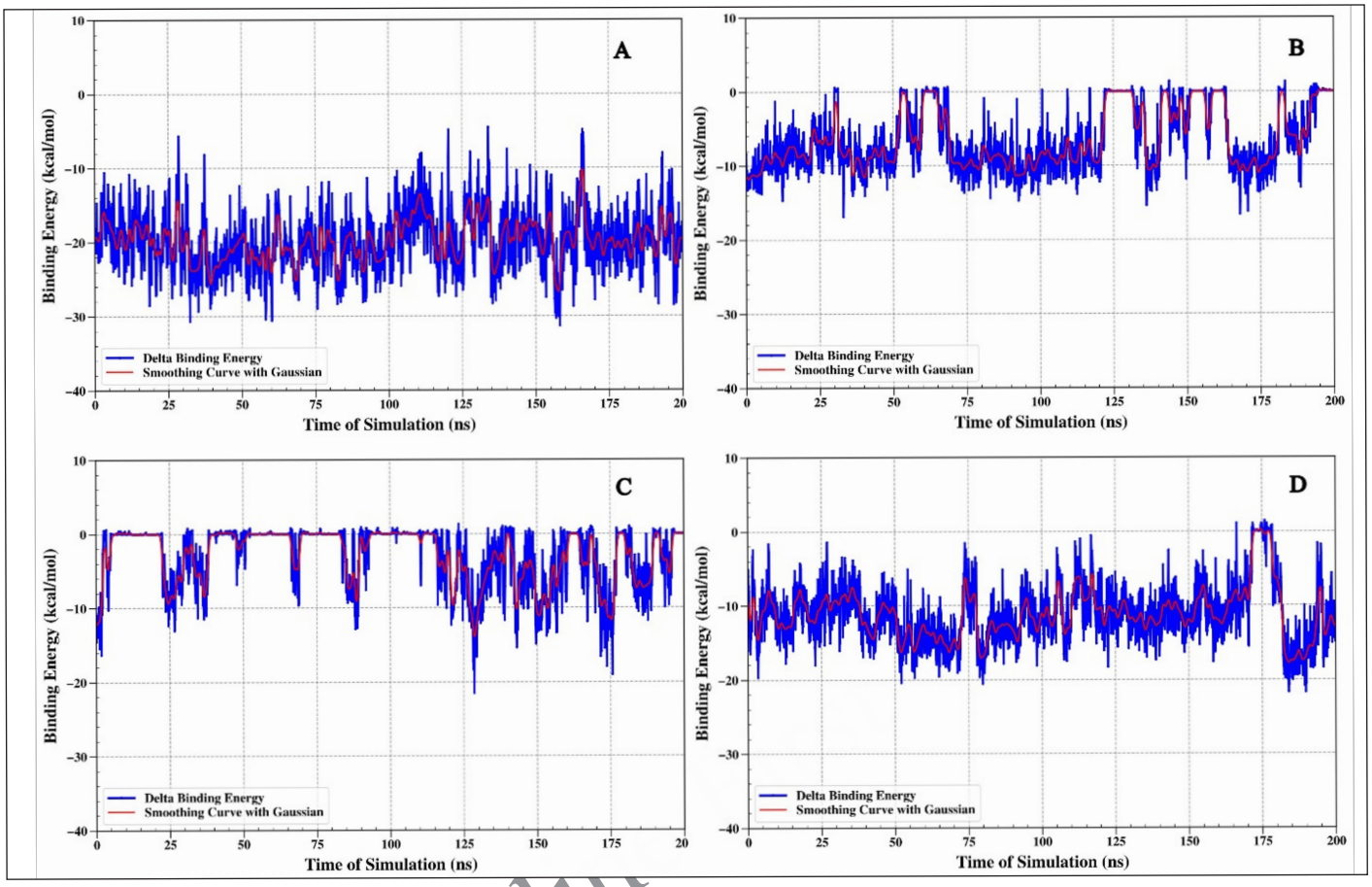

Figure 6. Binding energy analysis using the MMGBSA method was conducted for the TNF alpha–ligand complex, referred to as complex I.L6-1-(14-methylhexadecanoyl) pyrrolidine (A), IL6-7-hydroxy-6-methoxy-2H-chromen-2-one (B), IL6-N, N-dimethyltryptamine (C), and IL6-omeprazole (D).

shown in Figure 6. The ligand 1-(14-methylhexadecanoyl) pyrrolidine, which had a steady distance before, also shows a stable binding energy of about −20 kcal/mol (Fig. 6A). The ligand 1-(14-methylhexadecanoyl)pyrrolidine, which previously demonstrated a consistent distance, also exhibits a stable binding energy that remains approximately −20 kcal/mol (Fig. 6A). The binding energy consistently remains negative throughout the 200-ns simulation period. Such behavior suggests a robust and consistent binding affinity of this ligand to the TNF alpha protein.

Distance analysis on protein IL6

The outcomes of the molecular dynamics simulations of four IL6-ligand protein complex systems demonstrate markedly distinct interactions among the components. The observed pattern suggests that the chemical 7-hydroxy-6-methoxy-2H-chromen-2-one is likely to exhibit a strong affinity for the 1L6 protein. Simultaneously, the N,N-Dimethyltryptamine ligand (Fig. 7C) exhibits interaction features akin to those of the molecule 1-(14-methylhexadecanoyl)pyrrolidine (Fig. 7A), characterized by significant fluctuations in the relative pose distance of the ligand, which consequently influences the protein–ligand distance. The fluctuation pattern varies from 10 to 50 Å. The way the 1-(14-methylhexadecanoyl)pyrrolidine ligand and the N,N-dimethyltryptamine ligand attach to the protein changes, moving away and then coming back repeatedly. This pattern recurs. Despite the suspected weakness of the binding, this pattern indicates that both ligands exert a sufficient disruptive effect on the IL-6 protein, preventing super-inflammation.

MMGBSA: binding energy analysis on protein IL6

The binding energy study was done using the MMGBSA method for the four protein (IL6)–ligand complex systems showed results that matched what we found from the distance analysis. The ligands 1-(14-methylhexadecanoyl) pyrrolidine (Fig. 8A) and N,N-dimethyltryptamine (Fig. 8C) showed energy changes between −15 kcal/mol and 0. Negative binding energy values indicate that the ligand is associated with the protein.

In vivo validation

In vivo validation was carried out through a series of tests, following gastric lesion measurement, histopathology observation, immunohistochemistry analysis, and determination of IL-6 and TNF-α levels. The results of the tests are available on Figure 9.

The measurement of lesion surface area was performed to observe the severity of the gastric lesion in each

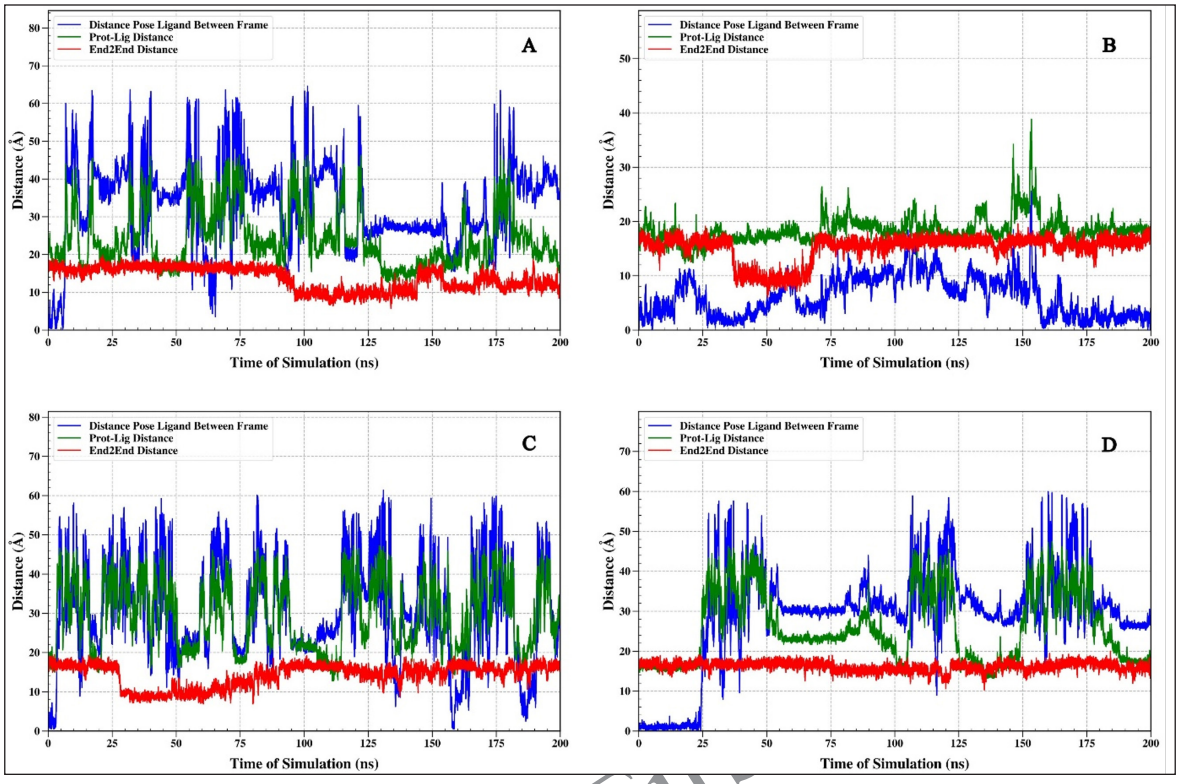

Figure 7. Analysis of distance between IL6 protein and ligand (green), end-to-end distance (red), and relative ligand position (blue) throughout a 200 ns molecular dynamics simulation. Complexes analyzed include: IL6-1-(14-methylhexadecanoyl)pyrrolidine (A), IL6-7-hydroxy-6-methoxy-2H-chromen-2-one (B), IL6-N,N-dimethyltryptamine (C), and IL6-omeprazole (D).

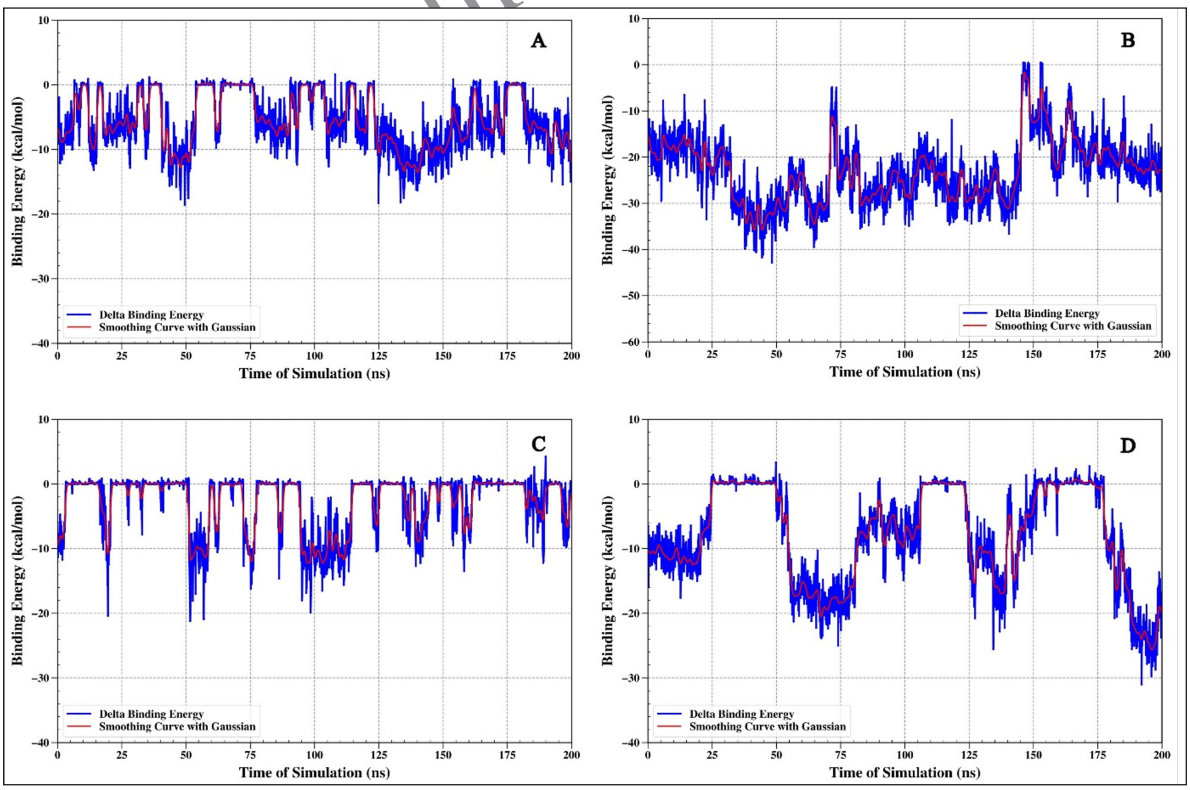

Figure 8. Binding energy analysis using the MMGBSA method for the protein (IL6)–ligand complex. Complex IL6-1-(14-methylhexadecanoyl) pyrrolidine (A), IL6-7-hydroxy-6-methoxy-2H-chromen-2-one (B), IL6-N,N-Dimethyltryptamine (C), and IL6-omeprazole (D).

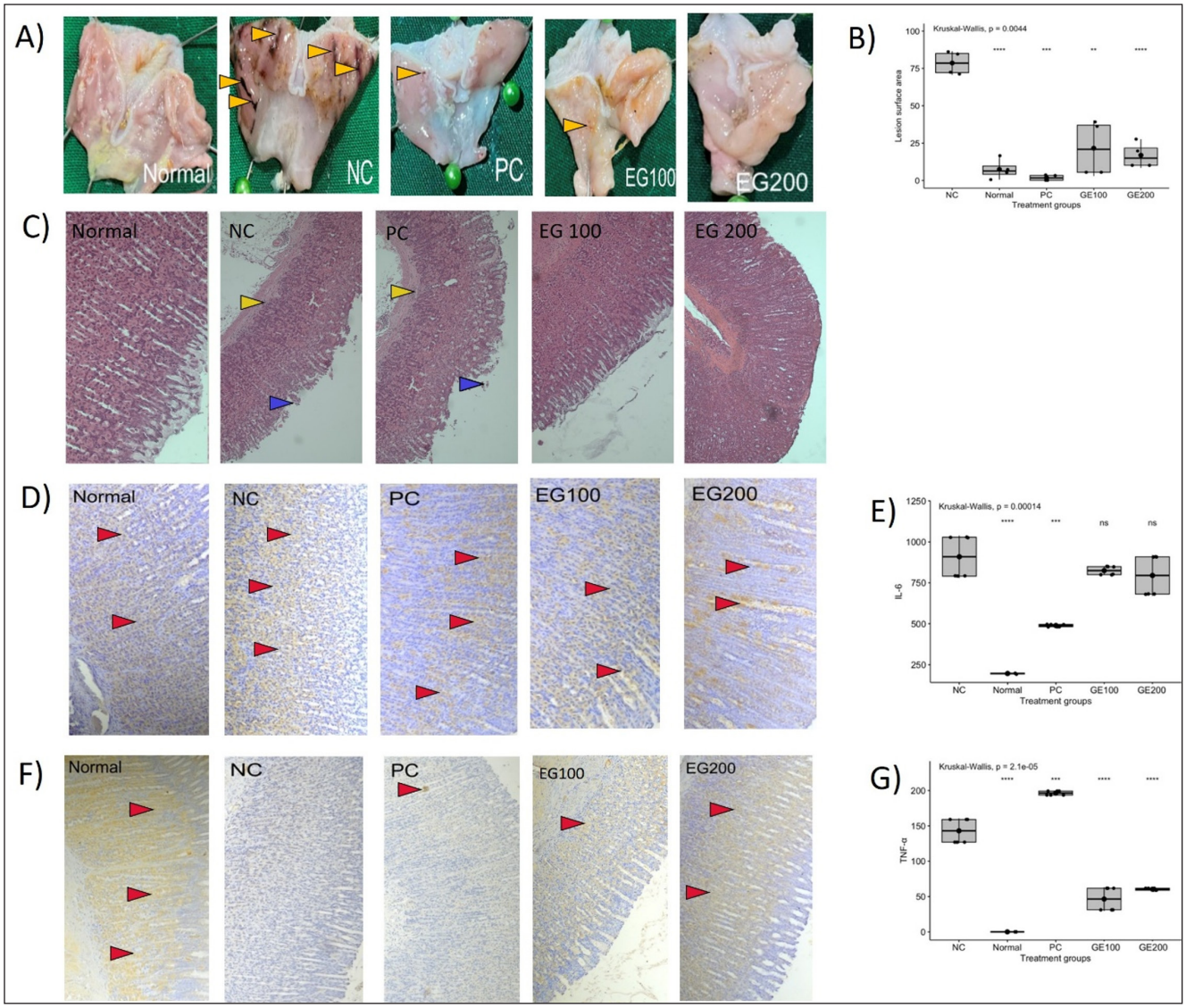

Figure 9. Results of *in vivo* assay in rats. Normal, NC = Negative control, PC = Positive control, EG100 = Extract of gambir 100, EG200 = Extract of gambir 200. A: Macroscopic observation of gastric lesions, a yellow arrow (▶) indicates hemorrhage; B: Measurement of gastric lesion surface area; C: Histopathology of stomach tissue using H&E staining, a blue arrow (▶) indicating villi erosion, a yellow arrow (▶) indicating inflammatory cell infiltration; D: Immunohistochemical staining, a red arrow (▶) indicating IL-6 levels in stomach samples; E: ELISA assay indicating the level of pro-inflammatory cytokine IL-6; F: Immunohistochemical staining, red arrow (▶) indicating TNF-α levels in stomach samples; G: ELISA assay indicating the level of pro-inflammatory cytokine TNF-α.

group. The lesion surface area was measured in percentage, comparing the lesion surface area and the total surface area of the stomach samples. Based on the result, there were significant differences ($p < 0.05$) observed from all groups compared to the negative control group, the boxplot result shows that the normal group had the smallest surface area of lesions, followed by the *B. kalalawit* extract at a dose of 200 mg/kg BW, positive control, and *B. kalalawit* extract at a dose of 100 mg/kg BW. The measurement of surface area of lesions is presented in Figure 9B.

Gastric lesions were also measured microscopically. Microscopic lesions were observed using the histopathology method (Fig. 9A). Microscopic observation using the histopathology method shows that the negative control group shows erosion of the epithelial wall, showing no epithelial wall to be observed on the histopathology.

Immunohistochemistry analyses were performed to determine of the level of pro-inflammatory cytokines TNF-α and IL-6 in the stomach samples. This approach helps evaluate the effect of gambir active compounds directly on the levels of TNF-α and IL-6 in the stomach samples, which is the primary site affected by acute gastritis. Elevated levels of TNF-α and IL-6 are indicated more intense staining of the tissue. The results of immunohistochemistry assay of TNF-α and IL-6 in each group are presented in Figure 9D and F, respectively.

Levels of pro-inflammatory cytokines TNF-α and IL-6 were measured by ELISA to observe the effect of *B. kalalawit* extract toward the levels of pro-inflammatory cytokines. Based

on the results on Figure 4E and G, the level of pro-inflammatory cytokine TNF-α in all rats showed a significant difference compared to negative control, although the group administered with omeprazole (positive control) showed the highest level of TNF-α compared to all other groups. The normal group showed the lowest level of TNF-α, followed by groups administered with *B. kalalawit* extract, at a dose of 100, and 200 mg/kg BW, respectively. The result of the level of pro-inflammatory cytokine IL-6 showed that there were significant differences observed from positive control and normal group compared to the negative control group. However, no significant differences were observed from the groups administered with *B. kalalawit* extract at all doses compared to the negative control group.

Acute toxicity showed that rats that received oral administration of *B. kalalawit* ethanol extract in increasing doses up to 2,000 mg/kg body weight, no side effects or deaths were observed during the 24-hour period after administration. These results indicate that the average lethal dose (LD50) for *B. kalalawit* ethanol extract in rats is likely to exceed 2,000 mg/kg. According to existing literature, compounds that show LD50 values greater than 2,000 mg/kg body weight are usually classified as non-toxic substances. Therefore, *B. kalalawit* is safe to use as a gastroprotective agent.

DISCUSSION

Based on the LC-HRMS analysis of *B. kalalawit* extract, a total of 70 active compounds were obtained, with 6 of them acting as secondary metabolite compounds. The six secondary metabolite compounds were chosen to further observe their relationship with gastritis. These secondary metabolites were analyzed for their activities using a network pharmacology approach. Network pharmacology is a newly established technique in the world of comparative medicine and drug development. This method is developed based on the theory of an "active ingredient, target, and disease" interactive network [27], constructing the relationship between active ingredients of medicinal substances and disease targets. The active secondary metabolites, which included catechin, 4-Methoxy DMT, N,N-Dimethyltryptamine, [1-(14′-Methylhexadecanoyl) pyrrolidine], 7-Hydroxy-6-methoxy-2H-chromen-2-one, and (+)-Procyanidin B2 were further observed in network pharmacology and proven to be related with gastritis gene targets.

The flavonoid compounds found were catechin and (+)-Procyanidin B2. Catechin is known for its important role in oxidative stress to counterattack reactive oxygen species (ROS), interacting with proteins, lipids, and ions in the tissues [28]. Other than that, catechin also works with regulating acetylcholine (ACh). ACh works with suppressing the expression of NF-kB in immune cells and macrophages, inhibiting the synthesis of pro-inflammatory cytokines [29,30], which is crucial in the response of acute inflammation, involving innate immunity cells and protecting the cells from oxidation at the earliest time of inflammation. (+)-Procyanidin, the other flavonoid compound, works with decreasing the release of inflammatory cytokines and suppressing ferroptosis in the Nrf2/HO-1/Keap-1 pathway [31].

7-Hydroxy-6-methoxy-2H-chromen-2-one or known as scopoletin belongs to the classification of coumarin, known for its antioxidant, antimicrobial, and anti-inflammatory effect. The inflammation effect in coumarin works with suppressing the production of nitric oxide and prostaglandin E2 (PGE2), downregulating inducible nitric oxide synthase and COX-2, which in turn, alleviating inflammation, and tissue damage [32]. PGE2 and COX-2 are known for being actively produced in the early stages of inflammation, or in the acute phase [33].

4-Methoxy DMT and N,N-Dimethyltryptamine are secondary metabolites from plants with psychedelic properties. Several studies have shown the potential of psychedelic as anti-inflammatory substances [34,35]. [1-(14′-Methylhexadecanoyl) pyrrolidine] usually known as MQ-A_3 is usually found naturally in plants, its structure resembling amides and showing potentials in the process of biological signaling membrane cell [36].

Molecular docking on the active compounds of *B. kalalawit* extract, 7-hydroxy-6-methoxy-2H-chromen-and 1-(14-methylhexadecanoyl)pyrrolidine on TNF-α (PDB ID: 2AZ5) proved that the compounds had greater value of affinity energy compared to the native ligands of both proteins. This showed that both compounds have weaker potential for binding TNF-α compared to their native ligands [37]. Meanwhile, both compounds showed a strong inhibition potential on IL-6 as they showed higher affinity energy compared to their native ligands.

Hydrogen bonds and hydrophobic interaction are described as molecular interactions obtained from molecular docking visualization. A protein has its own active site, which is a receptor that can bind to a substrate, making it possible for ligand interaction. Interaction between the active site and ligand will inhibit receptor action due to the natural substrate not binding to the active site of the receptor. This causes inhibition of the receptor [38]. A hydrogen bond is a stabile bond that represents ligand interaction with TNF-α and IL-6, meanwhile, hydrophobic bond helped the confirmation of protein–ligand binding [39].

Active sites of IL-6 includes Phe74, Phe78, Leu178, Arg179, and Arg182 based on a study conducted by Tran *et al.* [17]. Based on the visualization created between IL-6 and omeprazole, only Leu178, Arg179, and Arg182 interacted through hydrogen bond. Three other amino acid residues also interacted with 1-(14-methylhexadecanoylpyrrolidine) and N,N-Dimethyltryptamine through hydrophobic interaction. Meanwhile, based on the visualization of IL-6 and 7-hydroxy-6-methoxy-2H-chromen-, only Arg179 and Arg182 interacted through hydrophobic interaction.

Active sites of TNF-α include Ser60, Leu120, and Tyr151 [40]. Visualization of TNF-α and omeprazole showed that only Tyr151 was bound with hydrogen interaction. The visualization of TNF-α with all test ligands of *B. kalalawit* extract active compounds showed hydrophobic interaction. Leu120 is an amino acid residue of TNF-α that interacted with all test ligands.

Based on the molecular docking, *B. kalalawit* extract showed only limited potentials for inhibiting TNF-α because of its weaker inhibition potential compared to omeprazole as a comparison ligand based on the affinity energy value obtained. Meanwhile, only 7-hydroxy-6-methoxy-2H-chromen- showed potential for inhibiting IL-6 because of its higher affinity energy compared to omeprazole. Based on the molecular dynamic, the ligand 1-(14-methylhexadecanoyl)pyrrolidine has a strong and stable connection with the TNF alpha protein, while the

ligand 7-hydroxy-6-methoxy-2H-chromen-2-one has a strong connection with the IL6 protein. Omeprazole, a commercial drug used as a comparison ligand, demonstrates significant binding capacity despite fluctuations in dynamics. The strength of omeprazole's interaction with TNF-α is weaker than that of 1-(14-methylhexadecanoyl)pyrrolidine, and its interaction with IL-6 is also weaker than that of 7-hydroxy-6-methoxy-2H-chromen-2-one.

Changes in the stomach structure caused by gastritis could be seen in the impairment of the gastric mucosal barrier, causing effects such as hemorrhagic injuries, and accumulative oxidative stress [41]. Gastric lesions can be classified into several types, such as crypt dilatation, submucosal fibrosis, adenomatous gastric hyperplasia, mineralization, and erosion or ulceration [42]. Lesions that can be observed macroscopically are erosion or ulceration, as measured in this parameter. Gastric ulcer is defined as acid-induced lesion in the stomach, characterized by the loss of mucosal integrity, sometimes extending into the submucosa or muscularis propria [43]. The negative control group showed loss of gastric mucosa integrity, indicated by dysplasia, along with epithelial erosion. Meanwhile, the positive control group and groups administered with *B. kalalawit* extract maintained their mucosal integrity.

The gastroprotective effect of *B. kalalawit* extract in reducing stomach lesion and structural disruption is due to its active compounds, which initiate a cascade of inflammatory reactions, stimulating the proliferation of pro-inflammatory cytokines that modulate inflammation. Research conducted by Gustia *et al.* [44], showed that gambir, at concentrations of 1, 10, and 100 µg/ml significantly increased the IL-6 levels in cells induced by lipopolysaccharide, highlighting the immunostimulant effect of gambir. At lower concentrations, gambir depresses the level of IL-6, and meanwhile, at a higher concentration, gambir works with elevating IL-6 level. This mechanism allows gambir to trigger an immune response against acute inflammation, explaining the reason for the elevated level of IL-6 despite some of its secondary metabolites working with depressing IL-6.

IL-6 is a soluble mediator with a pleiotropic effect in inflammation, immune response, and hematopoiesis [45]. As a major inducer of acute phase response, IL-6 acts as the body's innate reaction to infection or injury, serving as a messenger between the innate and adaptive immune responses, playing a role in gastritis-related inflammation [46]. During acute inflammation, blood cells such as monocytes, macrophages, and endothelial cells produce IL-6, promoting the recruitment of neutrophils through the activation of chemokines and adhesion molecules on endothelial cells, smooth muscle cells, and fibroblasts [47]. IL-6 has also been proven to prolong neutrophil survival through regulatory effects on the apoptosis of neutrophils [48].

Neutrophils release inflammatory factors and several cytokines that regulate inflammation and activate another type of immune cells, achieved through a hierarchy of chemotactic molecules, following chemoattractants such as chemokines or complement components. The process of chemotaxis is controlled by multiple intracellular signaling pathways (mitogen-activated protein kinase-dependent) [49]. IL-6 that works in prolonging neutrophil survival provides neutrophils with an extended period in managing acute inflammation in the system.

TNF-α is a cytokine that has been identified as a key regulator of inflammatory responses and is known to be involved in the pathogenesis of inflammatory response [50]. TNF-α is actively involved in the development of gastritis [51]. TNF-α works in two different pathways, which are the NF-κB and MAPK pathways. NF-κB pathway will induce NF-κB to translocate to the nucleus and promote the transcription of various inflammatory genes; meanwhile, the MAPK pathway contributes to the production of inflammatory mediators and promotes cell proliferation and differentiation.

The results showed that the level of TNF-α in groups administered with *B. kalalawit* extract was significantly lower compared to the normal group in ELISA assay but showed a high presence in immunohistochemistry assay. TNF-α is released by macrophages, dendritic, and lymphocytic cells during inflammation, and is also secreted by other cells such as mast cells, nerve cells, endothelial cells, lipocytes, and lymphocytes [52].

TNF-α acts as a key pro-inflammatory cytokine that binds to two different receptors, initiating signal transduction pathways, leading to cellular responses, such as cell survival, differentiation, and proliferation [53], including apoptosis or induction of cell death, programming cell death of infected or damaged cells [54]. However, TNF-α works better in chronic inflammation rather than acute inflammation [55]. This may explain the difference of TNF-α levels observed in the immunohistochemistry assay on the stomach tissue compared to the ELISA assay on blood sample; systemic inflammation is likely lower than the localized acute inflammation in the stomach. The inflammatory response might not have reached a systemic level yet.

While the TNF-α and IL-6 may help in alleviating inflammation, excessive level of TNF-α and IL-6 may lead to the accumulation of ROS, leading to oxidative stress and disruption of cellular homeostasis. However, the high antioxidant effect of *B. kalalawit* extract, proven by the result of DPPH analysis, which is at the value of 9.14 µg/ml may counteract excessive ROS in the body, preventing further cell damage, as expressed in the size of stomach lesions and histopathology of the stomach tissue. Based on Jumina *et al.* [56], an IC_{50} value that is below 50 µg/ml is categorized as a substance with very strong antioxidant activity.

Antioxidants work with counterattacking ROS, preventing excessive oxidative stress in the system and maintaining cellular redox homeostasis [57]. The antioxidant effect in *B. kalalawit* extracts prevents excessive ROS leading to uncontrolled damage in various cellular macromolecules [58], disruption of normal cellular function, inflammation, tissue injury, and organ dysfunction [59]. The strong antioxidant activity found in the *B. kalalawit* extract indicates potential protection against oxidative stress-mediated gastric mucosal damage. Oxidative stress plays an important role in the pathogenesis of gastritis by increasing lipid peroxidation and DNA damage that contribute to epithelial cell dysfunction and inflammation [60]. Antioxidant components in the *B. kalalawit* extract, such as flavonoids and

polyphenols, can neutralize ROS released by neutrophils and macrophages during the inflammatory process [61]. Correlation between antioxidant activity and anti-inflammatory effects has been reported in various experimental gastritis models [62]. Although we have not performed a formal correlation analysis between antioxidant IC50 values and cytokine levels, studies by Repetto and Llesuy [63] showed a significant inverse relationship ($r = -0.78$, $p < 0.01$) between antioxidant capacity and TNF-α levels in a rat gastritis model. Bai *et al*. [64], also reported that compounds with antioxidant activity can inhibit NF-κB activation, which is a major transcription factor regulating the expression of pro-inflammatory cytokine genes.

The binding affinity to IL-6 was higher compared to TNF-α, the *in vivo* results showed a significant reduction in TNF-α but not in IL-6. The phenomenon of discrepancy between *in silico* and *in vivo* can be explained by several factors. First, there are fundamental differences between *in silico* systems that model interactions of a single molecule with a single protein target and the complexity of *in vivo* biological systems involving pharmacokinetics, tissue distribution, and interactions with multiple targets [65]. Second, active compounds may undergo a metabolic transformation *in vivo* that alters their biological activity, as reported by Liu *et al.* [66] for flavonoid compounds. Third, inhibition of TNF-α production may occur through upstream regulation such as inhibition of NF-κB activation rather than direct interaction with the TNF-α protein [67]. The binding affinity values (−4.8 to −6.0 kcal/mol) are weaker compared to clinically approved inhibitors. This is a limitation of the study that needs to be acknowledged. However, natural compounds often work through multiple targets with synergistic effects that collectively provide significant therapeutic effects despite relatively moderate affinity for individual targets [68].

The disparity between systemic and local cytokine measurements presents a significant finding. Although serum ELISA revealed substantial TNF-α suppression without IL-6 modification, immunohistochemical tissue analysis showed diminished expression of both cytokines. Fundamental differences between local and systemic inflammation can explain this discrepancy. Immunohistochemistry detects protein expression at the local tissue level (gastric mucosa), while ELISA measures cytokine levels in the systemic circulation. The half-life of IL-6 is longer than TNF-alpha, 15.5 hours [69] compared to 14 minutes [70], so the levels of these cytokines in the blood may differ, where TNF-alpha decreases compared to IL-6. TNF-alpha itself increases the synthesis of anti-inflammatory factors, such as IL-10, corticosteroid, or prostanoids, which can negatively regulate its expression [71,72], so during certain periods, TNF-alpha levels in the blood decrease along with the negative feedback that occurs. At the tissue level, TNF-alpha production can be induced by inflammatory conditions and is autocrine [73], so its production in the intestinal mucosa continues for several periods. This is one of the factors that shows immunopositive reactions in gastric tissue.

There were some limitations in this research, including the absence of a toxicity test in the rats prior to the administration of the *B. kalalawit* extract. Further research should investigate the toxicity level of the *B. kalalawit* extract to determine its safety level prior to its use as a gastroprotective agent. These limitations provide important directions for future research to strengthen the scientific validity and translational value of our findings. Despite these limitations, our study provides valuable preliminary evidence for the potential therapeutic application of the studied *B. kalalawit* extract in gastritis treatment.

CONCLUSION

Bajakah kalalawit extract is proven to have a gastroprotective potential through network pharmacology and molecular docking approach, identifying the relation of its active secondary metabolite compounds and gene targets related to gastritis in human, confirmed further with *in vivo* analysis using rat models. Although this research has proven its effectivity, further assessment including safety level must be conducted in future research.

ACKNOWLEDGMENT

The authors would like to thank the Indonesian Ministry of Education, Culture, Research and Technology (Kemdikbudristekdikti) for funding the research through the BIMA Fundamental-Regular research (PFR), fiscal year 2024, No. 22010/IT.3D10/PT.01.03/P/B/2024.

AUTHOR CONTRIBUTIONS

All authors made substantial contributions to conception and design, acquisition of data, or analysis and interpretation of data; took part in drafting the article or revising it critically for important intellectual content; agreed to submit to the current journal; gave final approval of the version to be published; and agree to be accountable for all aspects of the work. All the authors are eligible to be an author as per the International Committee of Medical Journal Editors (ICMJE) requirements/guidelines.

CONFLICTS OF INTEREST

The authors report no financial or any other conflicts of interest in this work.

ETHICAL APPROVALS

The study protocol has been approved by the Ethics Committee of the School of Veterinary Medicine and Biomedical Sciences, IPB University, Indonesia (Approval No.: 237/KEH/SKE/ VIII/2024).

DATA AVAILABILITY

All data generated and analyzed are included in this research article.

PUBLISHER'S NOTE

All claims expressed in this article are solely those of the authors and do not necessarily represent those of the publisher, the editors and the reviewers. This journal remains neutral with regard to jurisdictional claims in published institutional affiliation.

USE OF ARTIFICIAL INTELLIGENCE (AI)-ASSISTED TECHNOLOGY

The authors declares that they have not used artificial intelligence (AI)-tools for writing and editing of the manuscript, and no images were manipulated using AI.

REFERENCES

1. Smith S, Muinah F, Rinaldo P. Infections with *Helicobacter pylori* and challenges encountered in Africa. World J Gastroenterol. 2019;25(25):3183–95. doi: https://doi.org/10.3748/wjg.v25.i25.3183
2. Miranda A, Caldato C, Said N, Levy S, Teixeira C, Quaresma S. Gender, age, endoscopic findings, urease and *Helicobacter pylori*: all uncorrelated within a sample of a high gastric cancer prevalence population in Amazon. Arq Gastroenterol. 2019;(6):264–69. doi: https://doi.org/10.1590/S0004-2803.201900000-50
3. Yuan S, Chen J, Ruan X, Sun Y, Zhang K, Wang X, *et al.* Smoking, alcohol consumption, and 24 gastrointestinal diseases: mendelian randomization analysis. Elife. 2023;12:e840519. doi: https://doi.org/10.7554/eLife.84051
4. Elseweidy MM. Brief review on the causes, diagnosis, and therapeutic treatment of gastritis disease. Altern Integr Med. 2017;6(1):231. doi: https://doi.org/10.4172/2327-5162.1000231
5. Chang W, Bai J, Tian S, Ma M, Li W, Yin Y, *et al.* Autophagy protects gastric mucosal epithelial cells from ethanol-induced oxidative damage via mTOR signaling pathway. Exp Biol Med. 2017;24:1025–33. doi: https://doi.org/10.1177/1535370216686221
6. Nam HH, Choo BK. *Geranium koreanum*, a medicinal plant Geranii Herba, ameliorate the gastric mucosal injury in gastritis-induced mice. J Ethnopharmacol. 2021;265:113041. doi: https://doi.org/10.1016/j.jep.2020.113041
7. Santos MP, Pereira JN, Delabio RW, Smith MAC, Payão SLM, Carneiro LC, *et al.* Increased expression of interleukin-6 gene in gastritis and gastric cancer. Braz J Med Biol Res. 2021;54(7):e10687. doi: https://doi.org/10.1590/1414-431X2020e10687
8. Kim JM, Kim SH, Ko SH, Jung J, Chun J, Kim N, *et al.* The guggulsterone derivative GG-52 inhibits NF-kB signaling in gastric epithelial cells and ameliorates ethanol-induced gastric mucosal lesions in mice. Am J Physiol Gastrointest Liver Physiol. 2014;304(2):193–202. doi: https://doi.org/10.1152/ajpgi.00103.2012
9. Garg V, Narang P, Taneja R. Antacids revisited: review on contemporary facts and relevance for self-management. Int J Med Res. 2022;50(3):3000605221086457. doi: https://doi.org/10.1177/03000605221086457
10. Kawashima R, Tamaki S, Kawakami F, Maekawa T, Ichikawa T. Histamine H_2-receptor antagonists improve non-steroidal anti-inflammatory drug-induced intestinal dysbiosis. Int J Mol Sci. 2020;21(21):8166. doi: https://doi.org/10.3390/ijms21218166
11. Elmahdy MF, Almater JS. Omeprazole induced increase in liver markers—a case report. J Clin Diagn Res. 2019;13(10):1–2. doi: https://doi.org/10.7860/JCDR/2019/41848.13218
12. Yibrin M, Oliveira D, Valera R, Pitt AE, Lutgen S. Adverse effects associated with proton pump inhibitor use. Cureus. 2021;13(1):e12759. doi: https://doi.org/10.7759/cureus.12759
13. Munggari IP, Kurnia D, Deawati Y, Julaeha E. Current research of phytochemical, medicinal, and non-medicinal uses of *Uncaria gambir* Roxb.: a review. Molecules. 2022;27(19):6551. doi: https://doi.org/10.3390/molecules27196551
14. Andre N, Wang X, He Y, Pan G, Kojo A, Liu Y. A review of the occurrence of non-alkaloid constituents in *Uncaria* species and their structure-activity relationships. Am J Biomed Life Sci. 2013;1:79–98. doi: https://doi.org/10.11648/j.ajbls.20130104.13
15. Ismail AS, Rizal Y, Armenia A, Kasim A. Identification of bioactive compounds in gambier (*Uncaria gambir*) liquid by-product in West Sumatra, Indonesia. Biodivers J. 2021;22(3):1474–80.
16. Windarsih A, Warmiko HD, Indrianingsih AW, Rohman A, Ulumuddin YI. Untargeted metabolomics and proteomics approach using liquid chromatography-orbitrap high resolution mass spectrometry to detect pork adulteration in *Pangasius hypopthalmus* meat. Food Chem. 2022;386:132856.
17. Tran QH, Nguyen QT, Vo NQH, Mai TT, Tran TTN, Tran TD, *et al.* Structure-based 3D-Pharmacophore modeling to discover novel interleukin 6 inhibitors: an *in silico* screening, molecular dynamics simulations and binding free energy calculations. PLoS One. 2022;17(4):1–21. doi: https://doi.org/10.1371/journal.pone.0266632
18. Salman HA, Yaakop AS, Aladaileh S, Mustafa M, Gharaibeh M, Kahar UM. Inhibitory effects of *Ephedra alte* on IL-6, hybrid TLR4, TNF-α, IL-1β, and extracted TLR4 receptors: *in silico* molecular docking. Heliyon. 2023;9(1):e12730. doi: https://doi.org/10.1016/j.heliyon.2022.e12730
19. Babalola S, Igie N, Odeyemi I. Molecular docking, drug-likeness analysis, *in silico* pharmacokinetics, and toxicity studies of p-nitrophenyl hydrazones as anti-inflammatory compounds against COX-2, 5-LOX, and H+/K+ ATPase. Pharm Front. 2022;4(4):250–66. doi: https://doi.org/10.1055/s-0042-1759688
20. Dallakyan S, Olson AJ. Small-molecule library screening by docking with PyRx. Methods Mol Biol. 2015;1263:243–50. doi: https://doi.org/10.1007/978-1-4939-2269-7_19
21. Dyas RAA, Wijianto BH. Docking studies for screening antibacterial compounds of Red Jeringau (*Acorus calamus* L.) using *Shigella flexneri* protein as a model system. Acta Chim Asiana. 2023;6(2):343–50. doi: https://doi.org/10.29303/aca.v6i2.161
22. Arifin WN, Zahiruddin WM. Sample size calculation in animal studies using resource equation approach. Malays J Med Sci. 2017;24(5):101–5. doi: https://doi.org/10.21315/mjms2017.24.5.11
23. Al-Quraishy S, Othman MS, Dkhil MA, Moneim AEA. Olive (*Olea europaea*) leaf methanolic extract prevents HCl/ethanol induced gastritis in rats by attenuating inflammation and augmenting antioxidant enzyme activities. Biomed Pharmacother. 2017;91:338–49.
24. Wafaey AA, El-Hawary SS, Mohamed OG, Abdelrahman SS, Ali AM, El-Rashedy AA, *et al.* UHPLC-QTOF-MS/MS profiling, molecular networking, and molecular docking analysis of *Gliricidia sepium* (Jacq.) Kunth. ex. Walp. stem ethanolic extract and its gastroprotective effect on gastritis in rats. Toxicol Rep. 2025;14:101944. doi: https://doi.org/10.1016/j.toxrep.2025.101944
25. Cavallini ME, Andreollo NA, Metze K, Araújo MR. Omeprazole and misoprostol for preventing gastric mucosa effects caused by indomethacin and celecoxib in rats. Acta Cir Bras. 2006;21:168–76. doi: https://doi.org/10.1590/s0102-86502006000300009
26. Lowry OH, Rosebrough NJ, Farr AL, Randall RJ. Protein measurement with the Folin phenol reagent. J Biol Chem. 1951;193(1):265–75.
27. Hopkins AL. Network pharmacology: the next paradigm in drug discovery. Nat Chem Biol. 2008;4:682–90.
28. Yang CS, Chen G, Wu Q. Recent scientific studies of a traditional Chinese medicine, tea, on prevention of chronic diseases. J Tradit Med Complement. 2014;4:17–23.
29. Kim JM, Heo HJ. The roles of catechins in regulation of systemic inflammation. Food Sci Biotechnol. 2022;31(8):957–70.
30. Shenhar-Tsarfaty S, Berliner S, Bornstein NM, Soreq H. Cholinesterases as biomarkers for parasympathetic dysfunction andinflammation-related disease. J Mol Neurosci. 2014;53:298–305.
31. Zeng J, Weng Y, Lai T, Chen L, Li Y, Huang Q, *et al.* Procyanidin alleviates ferroptosis and inflammation of LPS-induced RAW264. 7 cell via the Nrf2/HO-1 pathway. Naunyn-Schmiedeberg's Arch Pharmacol. 2024;397(1):4055–67.
32. Sakthivel KM, Vishnupriya S, Priya DLC, Rasmi RR, Ramesh B. Modulation of multiple cellular signalling pathways as targets for anti-inflammatory and anti-tumorigenesis action of Scopoletin. J Pharm Pharmacol. 2022;74(2):147–61.
33. Khan AA, Iadarola M, Yang HT, Dionne RA. Expression of COX-1 and COX-2 in a clinical model of acute inflammation. J Pain. 2007;8(4):349–54. doi: https://doi.org/10.1016/j.jpain.2006.10.004.
34. Flanagan TW, Nichols CD. Psychedelics as anti-inflammatory agents. Int Rev Psychiatry. 2018;30(4):363–75.
35. Flanagan TW, Billac GB, Landry AN, Sebastian MN, Cormier SA, Nichols CD. Structure–activity relationship analysis of psychedelics in a rat model of asthma reveals the anti-inflammatory pharmacophore. ACS Pharmacol Transl Sci. 2020;4(2):488–502.

36. Yajima A, Yabuta G. Synthesis and absolute configuration of MQ-A3 [1-(14'-methylhexadecanoyl) pyrrolidine], a novel aliphatic pyrrolidine amide from the tropical convolvulaceous species. Biosci Biotechnol Biochem. 2001;65(2):463–5.
37. Muhammad DBA, Zainul FM, Bintari YR. Studi *in silico*: potensi antibakteri senyawa aktif alga merah *Gracillaria verrucosa* untuk menghambat Penicillin Binding Protein (PBP) bakteri *Escherichia coli.* J Kedokt Komunitas. 2023;11(2):1–14. Available from: http://biosig.unimelb.edu.au/pkcsm/prediction
38. Ferdian PR, Elfirta RR, Ikhwani AZN, Kasirah K, Haerul H, Sutardi D, *et al.* Studi *in silico* senyawa fenolik madu sebagai kandidat inhibitor Mpro SARS-CoV-2. Media Penelit Pengemb Kesehat. 2021;31(3):213–32. doi: https://doi.org/10.22435/mpk.v31i3.4920
39. Fakhruri M, Rahmayanti Y, Isfanda. Potensi fitokimia *Citrus aurantum* (Hesperetin, naringenin) dalam menghambat xantin oxidase pada hiperurisemia secara *in silico*. J Heal Sains. 2021;2(1):79–89. doi: https://doi.org/10.46799/jhs.v2i1.80
40. Ha NX, Anh HTN, Khanh PN, Ha VT, Ha NV, Huong TT, *et al. In silico* and ADMET study of *Morinda longissima* phytochemicals against TNF-α for treatment of inflammation-mediated diseases. Vietnam J Chem. 2023;61(S1):57–63. doi: https://doi.org/10.1002/vjch.202200214
41. Liu J, Wang J, Shi Y, Su W, Chen J, Zhang Z. Short chain fatty acid acetate protects against ethanol-induced acute gastric mucosal lesion in mice. Biol Pharm Bull. 2017;40:1439–46. doi: https://doi.org/10.1248/bpb.b17-00240
42. Whary MT, Baumgarth N, Fox JG, Barthold SW. Biology and diseases of mice. In: Laboratory animal medicine. 3rd ed. Amsterdam, The Netherlands: Elsevier Science; 2015. pp. 43–149.
43. Narayanan M, Reddy KM, Marsicano E. Peptic ulcer disease and *Helicobacter pylori* infection. Mo Med. 2018;115:219–24.
44. Gustia E, Yufri A, Hefni D, Kamal S, Dachriyanus, Wahyuni FS. The immunostimulant activities of the Gambir (Uncaria gambir Roxb) on Raw 264.7 cell. Proceedings of the 2nd International Conference on Contemporary Science and Clinical Pharmacy 2021 (ICCSCP 2021); 2021 Oct 30–31; Padang, Indonesia. Paris: Atlantis press; 2021. Vol. 40, pp 282–8.
45. Tanaka T, Narazaki M, Kishimoto T. IL-6 in inflammation, immunity, and disease. Cold Spring Harb Perspect Biol. 2016;6(10): a016295.
46. Sánchez-Zauco N, Torres J, Gómez A, Camorlinga-Ponce M, Muãoz-Pérez L, Herrera-Goepfert R. Circulating blood levels of IL-6, IFN-γ, and IL-10 as potential diagnostic biomarkers in gastric cancer: a controlled study. BMC Cancer. 2017;17:1–10. doi: https://doi.org/10.1186/s12885-017-3310-9
47. Hunter CA, Jones SA. IL-6 as a keystone cytokine in health and disease. Nat Immunol. 2015;16(5):448–57.
48. Asensi V, Valle E, Meana A. *In vivo* interleukin-6 protects neutrophils from apoptosis in osteomyelitis. Infect Immun. 2004;72(7): 3823–8.
49. Kolaczkowska E, Kubes P. Neutrophil recruitment and function in health and inflammation. Nat Rev. 2013;13:159–75.
50. Bradley JR. TNF-Mediated inflammatory disease. J Pathol. 2008;214:149–60. doi: https://doi.org/10.1002/path.2287
51. Sitepu RR, Darmadi D, Siregar GA. Correlation between TNF-α and degree of gastritis. J Gastroenterol Hepatol Dig Endosc. 2018;19(1):16–9.
52. Ohkura N, Kitagawa Y, Sakaguchi S. Development and maintenance of regulatory T cells. Immunity. 2013;38:414–23.
53. Jang D, Lee A, Shin HY, Song H, Park J, Kang T, *et al.* The role of tumor necrosis factor alpha (TNF-α) in autoimmune disease and current TNF-α inhibitors in therapeutics. Int J Mol Sci. 2021;22(5):2719.
54. Van Loo G, Bertrand MJM. Death by TNF: a road to inflammation. Nat Rev Immunol. 2023;23:289–303.
55. Muth KN, Rech J, Losch FO, Hoerning A. Reversing the inflammatory process – 25 years of tumor necrosis factor-α inhibitors. J Clin Med. 2023;12(15):5039.
56. Jumina J, Siswanta D, Zulkarnain AK, Triono S, Priatmoko P, Yuanita E, *et al.* Development of C-Arylcalix[4]resorcinarenes and C-Arylcalix[4]pyrogallolarenes as antioxidant and UV-B protector. Indones J Chem. 2019;19(2):273.
57. Kozlov AV, Javadov S, Sommer N. Cellular ROS and antioxidants: physiological and pathological role. Antioxidants. 2024;13(5):602.
58. Ma Q. Transcriptional responses to oxidative stress: pathological and toxicological implications. Pharmacol Ther. 2010;125:376–93.
59. Hong Y, Boiti A, Vallone D, Foulkes NS. Reactive oxygen species signaling and oxidative stress: transcriptional regulation and evolution. Antioxidants. 2004;13(3):312. doi: https://doi.org/10.3390/antiox13030312
60. Kwiecien S, Jasnos K, Magierowski M, Sliwowski Z, Pajdo R, Brzozowski B, *et al.* Lipid peroxidation, reactive oxygen species and antioxidative factors in the pathogenesis of gastric mucosal lesions and mechanism of protection against oxidative stress-induced gastric injury. J Physiol Pharmacol. 2014;65(5):613–22.
61. Keyhanmanesh R, Boskabady MH, Eslamizadeh MJ, Khamneh S, Ebrahimi MA. The effect of thymoquinone, the main constituent of *Nigella sativa* on tracheal responsiveness and white blood cell count in lung lavage of sensitized guinea pigs. Planta Med. 2010;76:218–22. doi: https://doi.org/10.1055/s-0029-1186054
62. Kangwan N, Park JM, Kim EH, Hahm KB. Quality of healing of gastric ulcers: natural products beyond acid suppression. World J Gastrointest Pathophysiol. 2014;5(1):40–7.
63. Repetto MG, Llesuy SF. Antioxidant properties of natural compounds used in popular medicine for gastric ulcers. Braz J Med Biol Res. 2002;35(5):523–34.
64. Bai SK, Lee SJ, Na HJ, Ha KS, Han JA, Lee H, *et al.* β-Carotene inhibits inflammatory gene expression in lipopolysaccharide-stimulated macrophages by suppressing redox-based NF-κB activation. Exp Mol Med. 2005;37(4):323–34.
65. Sliwoski G, Kothiwale S, Meiler J, Lowe EW. Computational methods in drug discovery. Pharmacol Rev. 2014;66(1):334–95.
66. Liu H, Wu J, Chen H, Tang Y, Xue F, Wang Y. Predictive evaluation of intestinal absorption of flavonoids based on molecular weight and oral bioavailability. Food Funct. 2019;10(8):4991–5002.
67. Lawrence T. The nuclear factor NF-κB pathway in inflammation. Cold Spring Harb Perspect Biol. 2009;1(6):a001651.
68. Wagner H, Ulrich-Merzenich G. Synergy research: approaching a new generation of phytopharmaceuticals. Phytomedicine. 2009;16(2-3):97–110.
69. Kuribayashi T. Elimination half-lives of interleukin-6 and cytokine-induced neutrophil chemoattractant-1 synthesized in response to inflammatory stimulation in rats. Lab Anim Res. 2018;34:80–3.
70. Van Griensven M. Zytokine als Marker bei Polytrauma. Der Unf. 2014;117:699–702.
71. Beutler B, Krochin N, Milsark IW, Luedke C, Cerami A. Control of cachectin (tumor necrosis factor) synthesis: mechanisms of endotoxin resistance. Science. 1986;4753:977–80.
72. Ksontini R, MacKay SL, Moldawer LL. Revisiting the role of tumor necrosis factor alpha and the response to surgical injury and inflammation. Arch Surg. 1998;5:558–67.
73. Cairns CB, Panacek EA, Harken AH, Banerjee A. Bench to bedside: tumor necrosis factor-alpha: from inflammation to resuscitation. Acad Emerg Med. 2000;8:930–41.

How to cite this article:
Mustika AA, Sutardi LN, Andriyanto A, Aurellia S, Rahma A, Wiranti RW, Prawira AY, Jati DT, Handharyani E, Wahyudi ST. Therapeutic effects of *Bajakah kalalawit* extract (*Uncaria gambir* Roxb.) in HCl/ethanol-induced rats as an animal model in acute gastritis: UHPLC MS/MS profiling and *in vivo* approach with *in silico* validation. J Appl Pharm Sci. 2025. Article in Press.
http://doi.org/10.7324/JAPS3.2025.231503